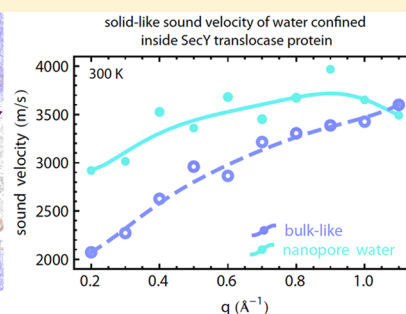
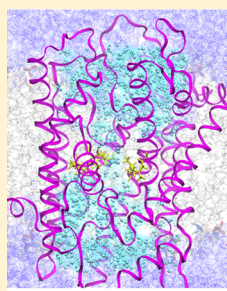


# Structural Relaxation Processes and Collective Dynamics of Water in Biomolecular Environments

Sara Capponi,<sup>\*,†,||</sup> Stephen H. White,<sup>†</sup> Douglas J. Tobias,<sup>‡,||</sup> and Matthias Heyden<sup>\*,§,||</sup><sup>†</sup>Department of Physiology and Biophysics and <sup>‡</sup>Department of Chemistry, University of California, Irvine, Irvine, California 92697-2025, United States<sup>§</sup>School of Molecular Sciences, Arizona State University, Tempe, Arizona 85287-1604, United States

## Supporting Information

**ABSTRACT:** In this simulation study, we investigate the influence of biomolecular confinement on dynamical processes in water. We compare water confined in a membrane protein nanopore at room temperature to pure liquid water at low temperatures with respect to structural relaxations, intermolecular vibrations, and the propagation of collective modes. We observe distinct potential energy landscapes experienced by water molecules in the two environments, which nevertheless result in comparable hydrogen bond lifetimes and sound propagation velocities. Hence, we show that a viscoelastic argument that links slow rearrangements of the water-hydrogen bond network to ice-like collective properties applies to both, the pure liquid and



biologically confined water, irrespective of differences in the microscopic structure.

## INTRODUCTION

The ability to form an extended and dynamic hydrogen bond (HB) network with a local tetrahedral structure, largely determines the properties of water.<sup>1–4</sup> In biomolecular systems water is often found in confining environments such as protein-binding pockets, membrane-protein channels, and narrow membrane pores.<sup>5,6</sup> Here, the restricted accessible volume along with surface effects influence water properties and result in characteristic differences to pure liquid water.<sup>7</sup> Water in such nano-confined environments contributes to the thermodynamics<sup>8</sup> and kinetics<sup>9</sup> of molecular recognition events. In some cases, water molecules constitute an integral part of a biomolecular structure or modulate functional dynamics.<sup>10</sup> Thus, to obtain a more complete understanding of complex biomolecular processes, detailed descriptions of confinement-mediated properties of water, its HB network structure and dynamics are needed. Relaxation processes of water can be probed by neutron spectroscopy,<sup>11</sup> dielectric spectroscopy,<sup>12</sup> or nuclear magnetic relaxation experiments.<sup>13,14</sup> Collective dynamics describing correlated motion of water molecules in time and space can be characterized with coherent scattering experiments.<sup>15,16</sup> All these experimental techniques report on averaged properties of water dynamics and structure, but lack the atomistic resolution necessary to resolve water properties in confined biomolecular environments. On the other hand, it is straightforward to obtain microscopic insights into local relaxation processes and collective dynamics from computer simulations.<sup>17–20</sup>

Neutron scattering studies have revealed that confined water at room temperature exhibits dynamics and a microscopic structure similar to supercooled bulk water, with a shift in temperature of  $\approx 30$  K.<sup>21,22</sup> Water confinement has also been exploited for studies of liquid water properties at supercooled temperatures because of the suppressed crystallization in confined environments.<sup>11,23</sup> In the present work, we study the relationship between structural rearrangements and collective dynamics of water confined in biomolecular environments using atomistic molecular dynamics (MD) simulations. Specifically, we go beyond earlier studies of water confined in idealized model systems<sup>24</sup> and examine the water-filled transmembrane nanopore of the biologically relevant SecY translocase<sup>25</sup> shown in Figure 1. We compare the properties of room temperature water confined in this nanopore to those of the pure liquid at low temperatures above the melting point of the respective water model. As expected, both confinement and reduced temperatures can result in an equivalent slow-down of the overall water HB network dynamics, as described, for example, by the average HB lifetime  $\tau_{\text{HB}}$ . An analysis of intermolecular vibrations reveals that distinct microscopic structures in confined and low temperature water give rise to the observed slow-down of HB dynamics. Despite these structural differences, we find that both environments have comparable effects on collective dynamics, such as sound propagation. In the protein nanopore and in the low

Received: December 14, 2018

Published: December 19, 2018

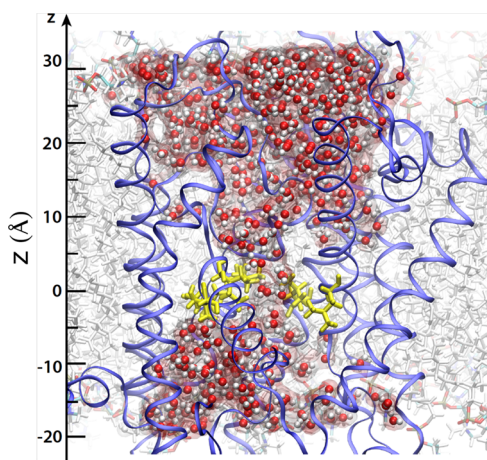


**Figure 1.** Representative snapshot of water (red and white van der Waals spheres and red transparent surface) confined inside SecY (blue ribbon representation). The hydrophobic residues delimiting the hydrophobic region (HR) are represented as yellow sticks; lipid tails in white; lipid headgroups in red, bronze, blue.

temperature water, the slowdown of structural relaxations results in fast sound propagation and the occurrence of dispersive transverse modes. Altogether we demonstrate that the viscoelastic argument, which relates structural relaxation processes in the HB network of pure water to collective properties of the liquid,<sup>26</sup> can be extended to water confined in biomolecular environments. This relationship provides an important link between local dynamical processes in water, which are accessible with spatial resolution in selected experiments,<sup>27</sup> and collective dynamics that are typically only observed as sample averages.

## METHODS

**Simulation Protocol of Water Confined in SecY.** As shown in Figure 1, the SecY translocase forms a large hourglass-shaped membrane nanopore that contains up to 400 water molecules and mediates the secretion or membrane-insertion of proteins. The protocol followed to set up and run the MD simulations is described in detail elsewhere.<sup>28</sup> Briefly, the SecY *Pyrococcus furiosus* crystal structure (PDBID: 3MP7)<sup>25</sup> used in the simulations describes an open state of the protein nanopore. We embedded the system in a POPC bilayer, performed an energy minimization followed by an equilibration and a subsequent 450 ns simulation in the *NPT* ensemble. The SecY cavity bottleneck is characterized by a HR, which is stable on the simulation timescale and is occupied by fluctuating numbers of water molecules.<sup>28</sup> From the 450 ns simulation, we extracted 24 independent configurations in which the SecY nanopore remains filled with water and free of lipid tail incursions. These configurations were used to start short (50 ps) simulations in the *NVE* ensemble that allowed us to examine in detail water dynamics inside the SecY nanopore. For our analysis, we report averages over these *NVE* simulations. To monitor how confinement affects the dynamic properties of water upon approaching the bottleneck of the SecY cavity, we defined a square prism region of  $40 \times 40 \times 100 \text{ \AA}^3$  enclosing the nanopore, divided it into 20 slabs of 5 Å thickness, and analyzed water molecules in each slab. All simulations were carried out with the NAMD software package<sup>29,30</sup> version 2.9. We employed the CHARMM36<sup>31</sup>

force field for the lipids, CHARMM22 with CMAP correction for the protein and ions,<sup>32,33</sup> and the TIP3P model<sup>34</sup> for water.

**Simulation Protocol of Bulk Water.** We compared the dynamic properties of water within SecY to the pure liquid at temperatures between 150 and 350 K. For this, we prepared a system of bulk TIP3P water containing 6845 water molecules in a cubic box with 60 Å edges for simulations at different temperatures. After performing an energy minimization, we equilibrated the system in the *NPT* ensemble at constant pressure of 1 bar and constant temperature *T*. We varied the temperature in 25 K steps between 150 and 350 K, so that 9 distinct temperatures were studied in total. The length of the *NPT* simulations varied with temperature in order to allow for a complete relaxation of the simulated water box (from 70 ns for the lowest temperatures to 15 ns for the highest temperature). We used the NAMD 2.9 software.<sup>29,30</sup> After equilibration, we ran *NVT* simulations of varying length for each temperature (between 5 and 20 ns for the highest and lowest temperatures, respectively), from which we extracted 5 independent configurations. The latter were then used as starting points for *NVE* simulations. The length of the *NVE* simulations was varied between 100 ps for the lowest temperatures and 50 ps for the highest; the coordinates and velocities were saved every 5 fs. Simulations at 200 K were eventually used for the comparison of bulk water collective properties to water confined in the protein nanopore at room temperature, that is 300 K. The melting temperature of TIP3P water is only 146 K.<sup>35</sup> Our simulations at 200 K are therefore comparable to cold liquid water with a temperature above the melting point, not supercooled water.

**Water Model Dependence.** To test for the dependence of our observations on the particular simulation model, we carried out additional simulations with the TIP4P/2005 water model.<sup>36</sup> To compare to our results of TIP3P water confined inside the SecY nanopore, we substituted water molecules in the selected starting configurations of the SecY system previously described and re-equilibrated the systems for 10 ps prior to starting the *NVE* production simulations. In addition, we carried out bulk water simulations at selected temperatures following the protocol described for TIP3P.

The melting point of TIP4P/2005 water ( $T_m = 249 \text{ K}$ <sup>37</sup>) is significantly higher than that for TIP3P. Because of this difference in  $T_m$ , we use a bulk water temperature of 250 K for the comparison of pure low temperature water with water in biomolecular confinement at 300 K for simulations with the TIP4P/2005 water model. As for our simulations with the TIP3P model, this temperature is above the melting temperature and the liquid state is thermodynamically stable.

**HB Network Dynamics.** In both confined and bulk water, we studied the rearrangements of the HB networks in terms of the autocorrelation function  $c(t)$  of the HB population operator  $h(t)$ <sup>38,39</sup>

$$c(t) = \langle h(0)h(t) \rangle / \langle h^2 \rangle \quad (1)$$

$h(t)$  is equal to 1 if a donor–acceptor (D–A) pair is hydrogen bonded at time  $t$ , and 0 otherwise. We define the HB through a geometric criterion, for which the D–A distance is less than 3.5 Å and the D–H–A angle is greater than 150°. The  $c(t)$  functions provide information on the lifetime of the local water HB network by taking into account the reformation of transiently broken HBs.

**Velocity Autocorrelation Functions and Vibrational Density of States.** In both confined and bulk water, we

computed the normalized water oxygen and water hydrogen velocity autocorrelation functions (VACF) as

$$C_{vv}(t) = \frac{\langle \mathbf{v}(t) \cdot \mathbf{v}(0) \rangle}{\langle \mathbf{v}(0) \cdot \mathbf{v}(0) \rangle} \quad (2)$$

$\mathbf{v}(t)$  is the velocity of the particular atom at time  $t$ , the angular brackets denote the average over molecules and time origins. The VACF of water oxygens and hydrogens was computed for water in the protein nanopore and for water in the vicinity of the HR and was compared to the corresponding result for bulk water at temperatures of 150, 200, 225, and 300 K.

To characterize the spectra of intermolecular vibrations, we then computed the vibrational density of states (VDoS) of the water oxygen and hydrogen atoms as the Fourier transform of the VACF:<sup>40–42</sup>

$$\text{VDoS}(\omega) \propto \int_0^\infty e^{-i\omega t} C_{vv}(t) dt \quad (3)$$

**Collective Dynamics from Current Spectra.** We computed the longitudinal current spectra  $I^{\parallel}(q, \omega)$  and its transverse counterpart  $I^{\perp}(q, \omega)$  directly from space and time correlations of density currents, which we computed using the atomic velocities. We analyze longitudinal current spectra  $I^{\parallel}(q, \omega)$ , which contain information on collective dynamics and on the propagation of density fluctuations within the system. A detailed description of the protocol for this analysis is provided in the [Supporting Information](#).

## RESULTS & DISCUSSION

**HB Dynamics in Confined and Low-Temperature Water.** In [Figure 2a,b](#), we plot the HB correlation function

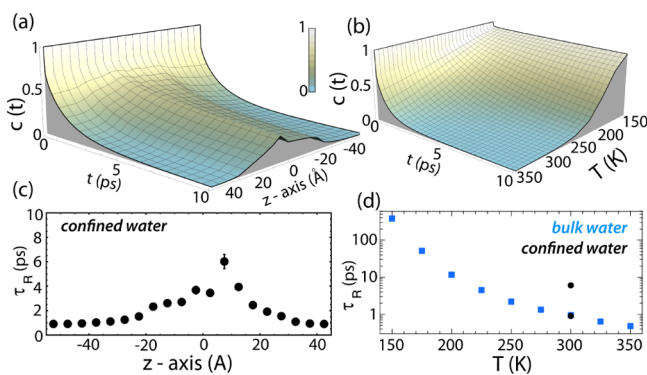


**Figure 2.** HB time correlation functions,  $c(t)$ , for water in SecY as a function of position  $z$  along the membrane normal in the nanopore (a) and in pure water as a function of temperature (b). The corresponding lifetimes  $\tau_{\text{HB}}$  are shown in panels (c,d). For pure water at 150 K, an extrapolation is used to estimate  $\tau_{\text{HB}}$  outside the analyzed correlation time window. In panel (d), blue square symbols represent HB lifetimes in pure water, while black circles provide a comparison to the slowest and fastest HB lifetimes from panel (c).

$c(t)$  of water within the SecY nanopore at 300 K as a function of position along the  $z$ -axis (normal to the membrane plane) and of pure water at varying temperatures. The corresponding average HB lifetimes  $\tau_{\text{HB}}$  are shown in [Figure 2c,d](#), which were defined for simplicity as  $c(\tau_{\text{HB}}) = e^{-1}$ .

Upon approaching the nanopore bottleneck, the HB network average lifetime in confined water increases from  $\tau_{\text{HB}} \approx 1$  ps for  $|z| > 30$  Å (bulk-like) to  $\approx 6$  ps for  $z \approx 5$  Å close to the HR of the SecY nanopore ([Figure 2c](#)). A comparable

increase of  $\tau_{\text{HB}}$  by 5 ps is observed for pure TIP3P water upon cooling to 200–225 K ([Figure 2d](#)), which is consistent with experiments carried out on water confined in porous materials and on supercooled water.<sup>21,22</sup> In earlier simulations with the SPC/E<sup>43</sup> water model, Starr et al.<sup>44</sup> observed a 5 ps increase of the structural relaxation time  $\tau_{\text{R}}$  (defined equivalently to  $\tau_{\text{HB}}$ ) upon cooling from 300 to 275 K. In the present study, we used the TIP3P<sup>34</sup> water model for which the employed protein and lipid force field was parametrized. Both water models, TIP3P and SPC/E, were fitted to reproduce only room temperature properties of water. As a consequence, the TIP3P water model yields a melting point of 146 K<sup>35</sup> and the SPC/E water model has a melting point of 215 K.<sup>35</sup> Therefore, we find for both models that relative to their respective melting points, the 5 ps increase in the HB network rearrangement time occurs for comparable degrees of cooling, corresponding to low temperature water above the melting point, not supercooled water.

Overall, we find that confinement and low temperatures can yield comparable effects on HB network dynamics. Although we expected this result, given previous work,<sup>28,45,46</sup> we suspected that the mechanisms underlying the slowdown of dynamics are different. In pure water, the decrease in thermal energy associated with cooling reduces the probability to overcome kinetic barriers involved in HB network rearrangements. The average water structure also experiences changes with temperature<sup>47,48</sup> resulting in variations of the intermolecular interactions. The local tetrahedral structure remains intact and is expected to be more pronounced at low temperature. Conversely, in a confining biomolecular environment the interactions with the protein surface, sterical constraints, and local differences in the solvent structure modify simultaneously the shape of the potential energy surface that determines HB dynamics.

**Spectrum of Intermolecular Vibrations.** To characterize potential energy landscapes experienced by water molecules within the translocon nanopore and in the pure liquid over a range of temperatures, we analyzed intermolecular vibrations on the subpicosecond and picosecond timescale. In [Figure 3](#), we focus on vibrations of water oxygen atoms, which dominate the low-frequency vibrations relevant for relaxation processes and density fluctuations. A corresponding analysis for water hydrogens is shown in the [Supporting Information](#) ([Figure S1](#)). [Figure 3a](#) shows that the structuring of the oxygen water VACF in pure water increases with decreasing temperature. For water at 300 K, the VACF features no significant minima or maxima, but instead decays to zero almost monotonically with a shoulder at  $\approx 130$  fs. In contrast, well-defined minima and maxima appear for lower temperatures and are most pronounced at the lowest temperature of 150 K. The period of the visible oscillations allows us to infer a dominant frequency around  $250 \text{ cm}^{-1}$ , reminiscent of HB stretch vibrations in water.<sup>49</sup> Indeed, the corresponding VDoS in [Figure 3b](#) shows a continuous increase in intensity of a broad vibrational band between 200 and  $300 \text{ cm}^{-1}$  with decreasing temperature. The integrated intensity of the VDoS describes the total number of degrees of freedom and is therefore constant. The increased VDoS between 200 and  $300 \text{ cm}^{-1}$  for low-temperature water is compensated by a loss of low frequency modes  $< 50 \text{ cm}^{-1}$  and diffusive degrees of freedom ( $0 \text{ cm}^{-1}$ ). The latter is closely tied to the increase in structural relaxation times as reported in [Figure 2](#). In addition, the maximum of the prominent peak between 30 and  $80 \text{ cm}^{-1}$  of pure water, which reports on so-

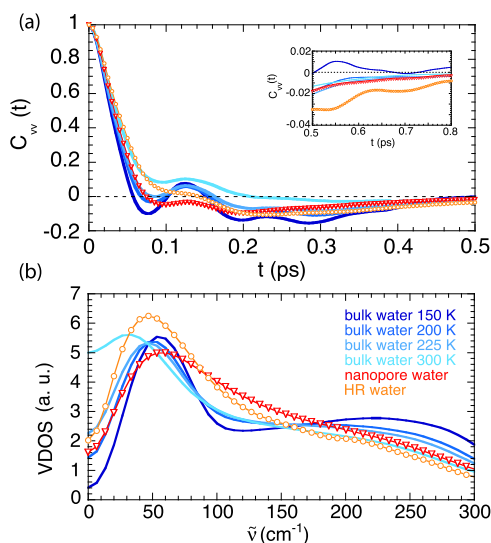


**Figure 3.** (a) Time evolution of normalized water oxygen velocity auto-correlation functions  $C_{vv}$  and (b) corresponding VDoS, as a function of wavenumbers. Solid lines represent results for pure water at 150 K (navy blue), 200 K (dark blue), 225 K (light blue), 300 K (cyan); red squares and orange circles describe data for nanopore and HR water, respectively.

called HB bending vibrations,<sup>49</sup> exhibits a pronounced blue-shift with decreasing temperature.

In the SecY simulation, we analyzed the difference between water confined in the nanopore and water confined in proximity of the HR region in order to monitor the effects of varying the degree of confinement. The HR region

corresponds to the bottleneck of the SecY nanopore. In contrast to low temperatures, biomolecular confinement within the SecY protein did not affect the HB stretch band of the water oxygen VDoS. In the corresponding VACF, a long-lasting, low intensity oscillatory feature for water oxygens near the HR region (inset of Figure 3) shows some similarity with water at 150 K. Other features including the 130 fs shoulder are significantly decreased in intensity. In both, the nanopore and the HR region, the water oxygen VACF exhibits a broad minimum with negative intensity following the fast sub 100 fs initial decay, before converging to zero for long correlation times. Interestingly, the initial fast decay of the VACF of water in the HR region follows the one observed for 300 K pure water, while the initial decay for all water molecules in the nanopore resembles the one of water at 225 K. In the VDoS, the mode density  $>200 \text{ cm}^{-1}$  for water in the protein nanopore and in the HR region is comparable to the pure liquid at 300 K. Instead, an increased number of modes is found at intermediate frequencies between 80 and  $200 \text{ cm}^{-1}$  in addition to the expected loss of diffusive modes at zero frequency. For water oxygens in the HR region, the intensity of the HB bending band ( $50 \text{ cm}^{-1}$ ) increases, which is not observed for the average of the entire nanopore.

Overall, decreased structuring of the VACF and a broader distribution of vibrational frequencies in the VDoS of confined water molecules in the protein indicates averaging over a heterogeneous mix of local environments.<sup>50</sup> This is clearly distinct from pure water at low temperatures, for which the increase of high frequency HB stretch vibrations in the VDoS and the structuring of the VACF indicate a strengthening of

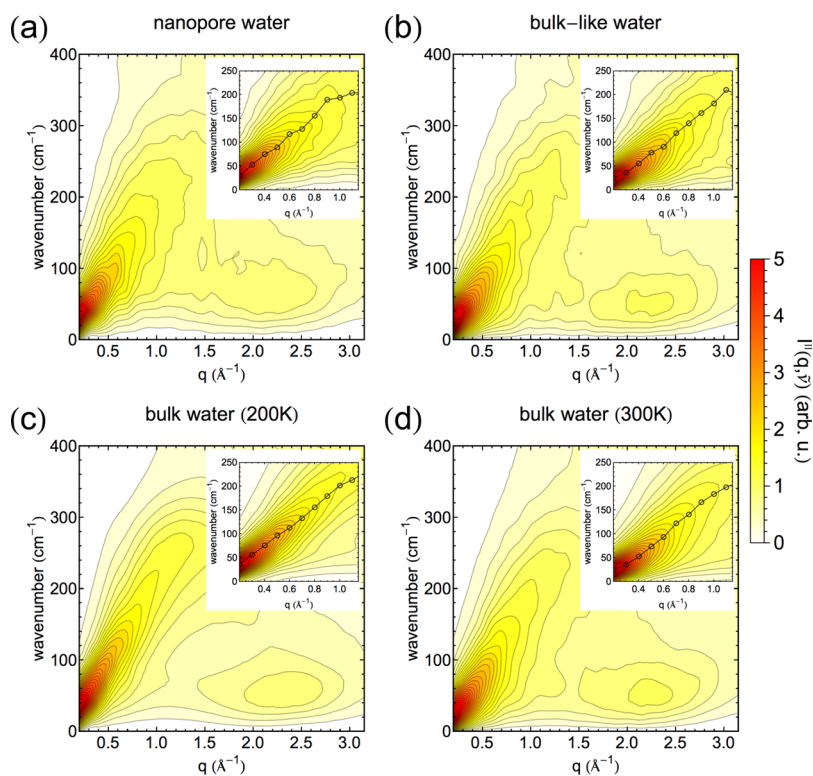


**Figure 4.** Longitudinal current spectra as a function of the scattering vector length  $q$  and the frequency in wavenumbers  $\tilde{\nu} = \omega/(2\pi c)$  of (a) water molecules inside the SecY nanopore, of (b) bulk-like water of the SecY simulation, of (c) pure water at 200 K, and (d) 300 K. Insets: longitudinal current spectra for  $q$  between  $0.2$  and  $1.1 \text{ \AA}^{-1}$  along with the  $q$ -dependent collective mode frequency.

the HB network and increasingly homogeneous local environments for water molecules.

**Collective Dynamics.** A major focus of this work is the influence of biomolecular confinement on collective dynamics and its relation to structural relaxation processes as described by HB correlation functions. Variations in the propagation of density fluctuations investigated here do not imply changes in the average structure, but can be modulated by them. In Figure 4, we show the longitudinal current spectra  $I^{\parallel}(q, \omega)$  computed from the space and time correlations of atomic velocities (see Supporting Information). These spectra characterize propagating acoustic modes and relate to the dynamic structure factor observed in coherent scattering experiments. We compared the collective dynamics of pure water as a function of temperature and of water confined within SecY. In the latter case, we focused our analysis on contributions from a given portion of the simulated system.<sup>17</sup> For this purpose, we computed cross correlations between current densities obtained for the entire simulated system and a selected set of water molecules, either within (nanopore water in Figure 4a) or outside (bulk-like water in Figure 4b) the SecY nanopore.

Generally, the longitudinal current spectrum  $I^{\parallel}(q, \omega)$  of pure water at room temperature describes a dispersive collective mode whose frequency depends on the momentum transfer  $q$ . We determined the  $q$ -dependent position of the dispersive mode  $\Omega(q)$  by fitting a two-damped harmonic oscillator model (see Supporting Information). For  $q < 0.2 \text{ \AA}^{-1}$ , that is large wavelengths that are not directly observed here as they extend beyond the size of the simulated systems, a propagation velocity  $c_0 = \Omega(q)/q = 1500 \text{ m/s}$  is expected, which corresponds to the ordinary sound velocity of water.<sup>51</sup> Further, no collective modes of transverse character are expected, which are symmetry-forbidden in liquids. However, early simulations and following experiments have shown that for shorter wavelengths, that is  $q > 0.2 \text{ \AA}^{-1}$  and within the detectable range of wavelengths in our simulation, the collective mode frequency increases with a distinct slope suggesting the occurrence of “fast” sound propagating with  $c_{\infty} > 3000 \text{ m/s}$ .<sup>18,26,52,53</sup> The latter roughly corresponds to the sound propagation velocity in ice. In Figure 5, we plot the

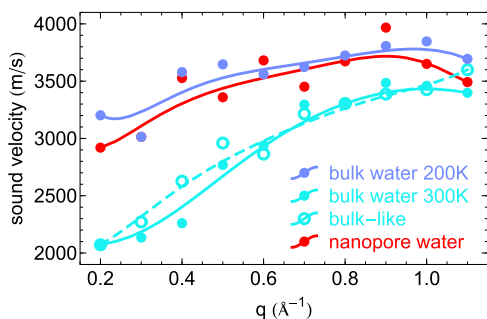


**Figure 5.** Apparent  $q$ -dependent sound velocities of water in distinct environments. Spline functions provide a guide to the eye.

apparent propagation velocities  $c(q) = \Omega(q)/q$  of each analyzed water species. The transition from almost ordinary sound velocities  $c(q) = \Omega(q)/q = 2000 \text{ m/s}$  at  $q = 0.2 \text{ \AA}^{-1}$  to fast sound of  $3500 \text{ m/s}$  at  $q > 0.7 \text{ \AA}^{-1}$  is observed in the room temperature simulations for pure water and bulk-like water outside the protein nanopore. Moreover, additional collective modes of transverse character can be observed at high  $q$  in

these cases (see Figure S2 in Supporting Information), which are only symmetry-allowed in solids.<sup>54</sup>

This behavior can be explained in terms of viscoelasticity. The collective mode frequencies at  $q < 0.2 \text{ \AA}^{-1}$  remain between  $0$  and  $20 \text{ cm}^{-1}$ . The corresponding timescales  $2\pi/\Omega(q)$  are  $>1.5 \text{ ps}$  and thus larger than the typical structural relaxation time in pure water of  $\tau_{\text{HB}} \approx 1 \text{ ps}$ . For larger momentum transfers  $q$ , the timescale associated with the mode frequency becomes shorter than  $\tau_{\text{HB}}$ . On this timescale, water essentially loses its liquid properties and resembles a solid, resulting in increased “solid-like” sound velocities and otherwise symmetry-forbidden transverse collective modes.<sup>54</sup> Alternative interpretations have been proposed, for example an interaction between dispersive ordinary sound modes with nondispersive intermolecular vibrations.<sup>55,56</sup> However, the temperature-dependence of the transition between ordinary and fast sound propagation in pure water supports the viscoelastic interpretation. With decreasing temperature, structural relaxation times in water increase significantly as shown in Figure 2 and the viscoelastic model predicts a transition between ordinary “liquid-like” and fast “solid-like” sound propagation at lower  $q$ -values and corresponding mode frequencies, which has been confirmed experimentally.<sup>26</sup>

Structural relaxation times in water confined within SecY are also increased relative to pure water at the same temperature (Figure 2). While the analysis in Figure 3 shows that the origin of slow dynamics in confined water is distinct from slow dynamics at low temperatures, our results show that the effects on collective dynamics are equivalent, that is we observe solid-like sound propagation at low  $q$  for water confined within the nanopore. For confined water and for pure water at  $200 \text{ K}$ , we find an essentially constant solid-like sound velocity  $>3000 \text{ m/s}$  within the entire analyzed  $q$ -range. Only for  $q < 0.3 \text{ \AA}^{-1}$ , we observe a beginning decrease toward a more liquid-like behavior. In accordance with solid-like collective dynamics for confined water and low temperature water, we also observe in both cases a dispersive mode of transverse symmetry at low  $q$  (see Supporting Information, Figure S2). Our control simulations with the TIP4P/2005 water model,<sup>36</sup> which offers an improved description of temperature-dependent water properties, confirm our general observations (see Figure S3 in Supporting Information).

Our results demonstrate that the viscoelastic mechanism can be applied in a similar way as in the pure liquid to relate local structural relaxations and collective dynamics for water confined in biomolecular environments. A slow-down of structural relaxation dynamics results in effectively solid-like properties on longer time- and length-scales in the protein nanopore, which results in solid-like fast sound propagation and transverse symmetry modes for lower  $q$ -values and frequencies than in pure and bulk-like water at room temperature. This specific behavior can be directly compared to the effect of lowering the temperature in pure water.

## CONCLUSIONS

Our results show that the slow-down of HB relaxation dynamics in water confined in the SecY membrane nanopore can be compared to the effect of decreased temperatures in pure water. Average HB lifetimes in the nanopore bottleneck at  $300 \text{ K}$  reflect the dynamics of pure water at  $200\text{--}225 \text{ K}$ , which is above the freezing point of the employed water model. In the SecY nanopore, geometrical constraints and interactions with the surrounding protein environment are responsible for slow

dynamics, while low temperatures in pure water mainly affect the ability to overcome kinetic barriers required to break individual HBs.

Despite similar dynamics, the potential energy surfaces experienced by confined or low temperature water molecules differ significantly, which becomes evident in the spectra of intermolecular vibrations. For pure low-temperature water, an increased number of high-frequency HB stretch vibrations indicates an increasingly tetrahedral structure. For confined water, we instead observe a wide distribution of vibrational frequencies between the water HB bending and HB stretching band. This result highlights potential pitfalls in comparing water in confined biomolecular environments to the bulk liquid at low temperatures.

However, we demonstrate that the same viscoelastic arguments can be used to predict the effects of confinement and low temperatures on collective water dynamics. In both cases, the slowdown in structural relaxation dynamics results in an onset of solid-like collective dynamics, that is fast sound propagation and transverse symmetry modes, at lower momentum transfers and frequencies and corresponding longer length- and time-scales. Local differences in the potential energy surface described by the VDoS are less relevant for sound propagation than the lifetime of structural motifs in the water HB network. Hence, we anticipate that frequently observed retardations of local structural relaxations at other confining biomolecular interfaces<sup>57–59</sup> will also result in solid-like collective properties on greater length- and time-scales than in pure water. As shown in previous work,<sup>19</sup> collective modes within the HB network of water in the vicinity of proteins are coupled to vibrations on the same timescale within the proteins. However, whether such coupled motion has a measurable impact on the stability, conformational dynamics or biological function of proteins is not clear at this time.

## ■ ASSOCIATED CONTENT

### Supporting Information

The Supporting Information is available free of charge on the ACS Publications website at DOI: 10.1021/acs.jpccb.8b12052.

Analysis protocol for collective dynamics; time evolution of normalized velocity auto-correlation functions  $C_{vv}$  of TIP3P water hydrogen atoms; simulated transverse current spectra of water molecules; apparent  $q$ -dependent sound velocities of water in distinct environments for simulations with the TIP4P/2005 water model (PDF)

## ■ AUTHOR INFORMATION

### Corresponding Authors

\*E-mail: sara.capponi@ucsf.edu (S.C.).

\*E-mail: heyden@asu.edu (M.H.).

### ORCID

Sara Capponi: 0000-0001-8117-7526

Stephen H. White: 0000-0001-8540-7907

Douglas J. Tobias: 0000-0002-6971-9828

Matthias Heyden: 0000-0002-7956-5287

### Present Address

<sup>||</sup>Cardiovascular Research Institute, Department of Pharmaceutical Chemistry, University of California, San Francisco, CA 94143, USA.

## Notes

The authors declare no competing financial interest.

## ■ ACKNOWLEDGMENTS

This research was supported by grants from the National Institute of Health (PO1 GM86685 to D.J.T. and S.H.W.) and (RO1 GM74637 to S.H.W.). M.H. was supported by the German National Academy of Science, Leopoldina. The simulations were performed on HPC at the University of California, Irvine, and on Stampede on Extreme Science and Engineering Discovery Environment, supported by the National Science Foundation (ACI-1053575). This work is supported by the Cluster of Excellence RESOLV (EXC 1069) funded by the Deutsche Forschungsgemeinschaft (M.H.).

## ■ REFERENCES

- (1) Chaplin, M. Water: its importance to life. *Biochem. Mol. Biol. Educ.* **2001**, *29*, 54.
- (2) Chaplin, M. Do we underestimate the importance of water in cell biology? *Nat. Rev. Mol. Cell Biol.* **2006**, *7*, 861.
- (3) Ball, P. Water as an Active Constituent in Cell Biology. *Chem. Rev.* **2008**, *108*, 74.
- (4) Debenedetti, P. G.; Klein, M. L. Chemical physics of water. *Proc. Natl. Acad. Sci. U.S.A.* **2017**, *114*, 13325–13326.
- (5) Rasaiah, J. C.; Garde, S.; Hummer, G. Water in Nonpolar Confinement: From Nanotubes to Proteins and Beyond. *Annu. Rev. Phys. Chem.* **2008**, *59*, 713.
- (6) Li, J.; Shaikh, S. A.; Enkavi, G.; Wen, P.-C.; Huang, Z.; Tajkhorshid, E. Transient formation of water-conducting states in membrane transporters. *Proc. Natl. Acad. Sci. U.S.A.* **2013**, *110*, 7696.
- (7) Molinero, V.; Kay, B. D. Preface: Special Topic on Interfacial and Confined Water. *J. Chem. Phys.* **2014**, *141*, 18C101.
- (8) Krepl, M.; Blatter, M.; Cléry, A.; Damberger, F. F.; Allain, F. H. T.; Sponer, J. Structural study of the Fox-1 RRM protein hydration reveals a role for key water molecules in RRM-RNA recognition. *Nucleic Acids Res.* **2017**, *45*, 8046–8063.
- (9) Setny, P.; Baron, R.; Michael Kekenes-Huskey, P.; McCammon, J. A.; Dzubiella, J. Solvent fluctuations in hydrophobic cavity–ligand binding kinetics. *Proc. Natl. Acad. Sci. U.S.A.* **2013**, *110*, 1197–1202.
- (10) Angel, T. E.; Gupta, S.; Jastrzebska, B.; Palczewski, K.; Chance, M. R. Structural waters define a functional channel mediating activation of the GPCR, rhodopsin. *Proc. Natl. Acad. Sci. U.S.A.* **2009**, *106*, 14367–14372.
- (11) Capponi, S.; Arbe, A.; Cervený, S.; Busselez, R.; Frick, B.; Embs, J. P.; Colmenero, J. Quasielastic neutron scattering study of hydrogen motions in an aqueous poly(vinyl methyl ether) solution. *J. Chem. Phys.* **2011**, *134*, 204906.
- (12) Cervený, S.; Alegría, A.; Colmenero, J. Universal features of water dynamics in solutions of hydrophilic polymers, biopolymers and small glass-forming materials. *Phys. Rev. E: Stat., Nonlinear, Soft Matter Phys.* **2008**, *77*, 031803.
- (13) Qvist, J.; Persson, E.; Mattea, C.; Halle, B. Time scales of water dynamics at biological interfaces: peptides, proteins and cells. *Faraday Discuss.* **2009**, *141*, 131–144.
- (14) Busselez, R.; Arbe, A.; Cervený, S.; Capponi, S.; Colmenero, J.; Frick, B. Component dynamics in polyvinylpyrrolidone concentrated aqueous solutions. *J. Chem. Phys.* **2012**, *137*, 084902.
- (15) Orecchini, A.; Paciaroni, A.; De Francesco, A.; Petrillo, C.; Sacchetti, F. Collective Dynamics of Protein Hydration Water by Brillouin Neutron Spectroscopy. *J. Am. Chem. Soc.* **2009**, *131*, 4664–4669.
- (16) Russo, D.; Laloni, A.; Filabozzi, A.; Heyden, M. Pressure effects on collective density fluctuations in water and protein solutions. *Proc. Natl. Acad. Sci. U.S.A.* **2017**, *114*, 11410–11415.

- (17) Nibali, V. C.; D'Angelo, G.; Paciaroni, A.; Tobias, D. J.; Tarek, M. On the coupling between the collective dynamics of proteins and their hydration water. *J. Phys. Chem. Lett.* **2014**, *5*, 1181–1186.
- (18) Tarek, M.; Tobias, D. J. Single-particle and collective dynamics of protein hydration water: A molecular dynamics study. *Phys. Rev. Lett.* **2002**, *89*, 275501.
- (19) Heyden, M.; Tobias, D. J. Spatial-Dependence of Protein-Water Collective Hydrogen-Bond Dynamics. *Phys. Rev. Lett.* **2013**, *111*, 218101.
- (20) Hong, L.; Jain, N.; Cheng, X.; Bernal, A.; Tyagi, M.; Smith, J. C. Determination of functional collective motions in a protein at atomic resolution using coherent neutron scattering. *Sci. Adv.* **2016**, *2*, e1600886.
- (21) Teixeira, J.; Zanotti, J.-M.; Bellissent-Funel, M.-C.; Chen, S.-H. Water in confined geometries. *Phys. B* **1997**, 234–236, 370.
- (22) Bellissent-Funel, M.-C. Structure of confined water. *J. Phys.: Condens. Matter* **2001**, *13*, 9165.
- (23) Cervený, S.; Mallamace, F.; Swenson, J.; Vogel, M.; Xu, L. Confined Water as Model of Supercooled Water. *Chem. Rev.* **2016**, *116*, 7608–7625.
- (24) Cicero, G.; Grossman, J. C.; Schwegler, E.; Gygi, F.; Galli, G. Water Confined in Nanotubes and between Graphene Sheets: A First Principle Study. *J. Am. Chem. Soc.* **2008**, *130*, 1871–1878.
- (25) Egea, P. F.; Stroud, R. M. Lateral opening of a translocon upon entry of protein suggests the mechanism of insertion into membranes. *Proc. Natl. Acad. Sci. U.S.A.* **2010**, *107*, 17182.
- (26) Ruocco, G.; Sette, F. The history of the “fast sound” in liquid water. *Condens. Matter Phys.* **2008**, *11*, 29–46.
- (27) Barnes, R.; Sun, S.; Fichou, Y.; Dahlquist, F. W.; Heyden, M.; Han, S. Spatially Heterogeneous Surface Water Diffusivity around Structured Protein Surfaces at Equilibrium. *J. Am. Chem. Soc.* **2017**, *139*, 17890–17901.
- (28) Capponi, S.; Heyden, M.; Bondar, A.-N.; Tobias, D. J.; White, S. H. Anomalous behavior of water inside the SecY translocon. *Proc. Natl. Acad. Sci. U.S.A.* **2015**, *112*, 9016–9021.
- (29) Kalé, L.; Skeel, R.; Bhandarkar, M.; Brunner, R.; Gursoy, A.; Krawetz, N.; Phillips, J.; Shinozaki, A.; Varadarajan, K.; Schulten, K. NAMD2: Greater Scalability for Parallel Molecular Dynamics. *J. Comput. Phys.* **1999**, *151*, 283.
- (30) Phillips, J. C.; Braun, R.; Wang, W.; Gumbart, J.; Tajkhorshid, E.; Villa, E.; Chipot, C.; Skeel, R. D.; Kalé, L.; Schulten, K. Scalable Molecular Dynamics with NAMD. *J. Comput. Chem.* **2005**, *26*, 1781.
- (31) Klauda, J. B.; Venable, R. M.; Freites, J. A.; O'Connor, J. W.; Tobias, D. J.; Mondragon-Ramirez, C.; Vorobyov, I.; MacKerell, A. D.; Pastor, R. W. Update of the CHARMM All-Atom Additive Force Field for lipids: Validation on Six Lipid Types. *J. Phys. Chem. B* **2010**, *114*, 7830.
- (32) MacKerell, A. D.; et al. All-Atom Empirical Potential for Molecular Modeling and Dynamics Studies of Proteins. *J. Phys. Chem. B* **1998**, *102*, 3586–3616.
- (33) Mackerell, A. D.; Feig, M.; Brooks, C. L. Extending the Treatment of Backbone Energetics in Protein Force Fields: Limitations of Gas-Phase Quantum Mechanics in Reproducing Protein Conformational Distributions in Molecular Dynamics Simulations. *J. Comput. Chem.* **2004**, *25*, 1400.
- (34) Jorgensen, W. L.; Chandrasekhar, J.; Madura, J. D.; Impey, R. W.; Klein, M. L. Comparison of simple potential functions for simulating liquid water. *J. Chem. Phys.* **1983**, *79*, 926.
- (35) Vega, C.; Sanz, E.; Abascal, J. L. F. The melting temperature of the most common models of water. *J. Chem. Phys.* **2005**, *122*, 114507.
- (36) Abascal, J. L. F.; Vega, C. A general purpose model for the condensed phases of water: TIP4P/2005. *J. Chem. Phys.* **2005**, *123*, 234505.
- (37) Conde, M. M.; Rovere, M.; Gallo, P. High precision determination of the melting points of water TIP4P/2005 and water TIP4P/Ice models by the direct coexistence technique. *The Journal of Chemical Physics* **2017**, *147*, 244506.
- (38) Luzar, A.; Chandler, D. Effect of Environment on Hydrogen Bond Dynamics in Liquid Water. *Phys. Rev. Lett.* **1996**, *76*, 928.
- (39) Luzar, A.; Chandler, D. Hydrogen-bond kinetics in liquid water. *Nature* **1996**, *379*, 55.
- (40) Choudhury, N.; Pettitt, B. M. Dynamics of Water Trapped between Hydrophobic Solutes. *J. Chem. Phys. B* **2005**, *109*, 6422–6429.
- (41) Chakraborty, S.; Sinha, S. K.; Bandyopadhyay, S. Low-Frequency Vibrational Spectrum of Water in the Hydration Layer of a Protein: A Molecular Dynamics Simulation Study. *J. Chem. Phys. B* **2007**, *111*, 13626.
- (42) Rocchi, C.; Bizzarri, A. R.; Cannistraro, S. Water dynamical anomalies evidenced by molecular-dynamics simulations at the solvent-protein interface. *Phys. Rev. E: Stat. Phys., Plasmas, Fluids, Relat. Interdiscip. Top.* **1998**, *57*, 3315.
- (43) Berendsen, H. J. C.; Grigera, J. R.; Straatsma, T. P. The missing term in effective pair potentials. *J. Phys. Chem.* **1987**, *91*, 6269–6271.
- (44) Starr, F. W.; Nielsen, J. K.; Stanley, H. E. Fast and slow dynamics of hydrogen bonds in liquid water. *Phys. Rev. Lett.* **1999**, *82*, 2294.
- (45) Bagchi, B. Water dynamics in the Hydration Layer around Proteins and Micelles. *Chem. Rev.* **2005**, *105*, 3197.
- (46) Moilanen, D. E.; Levinger, N. E.; Spry, D. B.; Fayer, M. D. Confinement or the Nature of the Interface? Dynamics of Nanoscopic Water. *J. Am. Chem. Soc.* **2007**, *129*, 14311–14318.
- (47) Soper, A. K. The radial distribution functions of water and ice from 220 to 673 K and at pressures up to 400 MPa. *Chem. Phys.* **2000**, *258*, 121–137.
- (48) Modig, K.; Pfrommer, B. G.; Halle, B. Temperature-dependent hydrogen-bond geometry in liquid water. *Phys. Rev. Lett.* **2003**, *90*, 075502.
- (49) Walrafen, G. E. Raman spectrum of water: transverse and longitudinal acoustic modes below  $\approx 300\text{ cm}^{-1}$  and optic modes above  $\approx 300\text{ cm}^{-1}$ . *J. Phys. Chem.* **1990**, *94*, 2237–2239.
- (50) Pattni, V.; Vasilevskaya, T.; Thiel, W.; Heyden, M. Distinct Protein Hydration Water Species Defined by Spatially Resolved Spectra of Intermolecular Vibrations. *J. Phys. Chem. B* **2017**, *121*, 7431–7442.
- (51) Sciortino, F.; Sastry, S. Sound propagation in liquid water: The puzzle continues. *J. Chem. Phys.* **1994**, *100*, 3881–3893.
- (52) Rahman, A.; Stillinger, F. H. Propagation of sound in water. A molecular-dynamics study. *Phys. Rev. A* **1974**, *10*, 368.
- (53) Teixeira, J.; Bellissent-Funel, M. C.; Chen, S. H.; Dorner, B. Observation of new short-wavelength collective excitations in heavy water by coherent inelastic neutron scattering. *Phys. Rev. Lett.* **1985**, *54*, 2681.
- (54) Sampoli, M.; Ruocco, G.; Sette, F. Mixing of Longitudinal and Transverse Dynamics in Liquid Water. *Phys. Rev. Lett.* **1997**, *79*, 1678–1681.
- (55) Petrillo, C.; Sacchetti, F.; Dorner, B.; Suck, J.-B. High-resolution neutron scattering measurement of the dynamic structure factor of heavy water. *Phys. Rev. E: Stat. Phys., Plasmas, Fluids, Relat. Interdiscip. Top.* **2000**, *62*, 3611–3618.
- (56) Sacchetti, F.; Suck, J.-B.; Petrillo, C.; Dorner, B. Brillouin neutron scattering in heavy water: Evidence for two-mode collective dynamics. *Phys. Rev. E: Stat., Nonlinear, Soft Matter Phys.* **2004**, *69*, 061203.
- (57) Pal, S. K.; Peon, J.; Zewail, A. H. Biological water at the protein surface: Dynamical solvation probed directly with femtosecond resolution. *Proc. Natl. Acad. Sci. U.S.A.* **2002**, *99*, 1763–1768.
- (58) Nucci, N. V.; Pometun, M. S.; Wand, A. J. Site-resolved measurement of water-protein interactions by solution NMR. *Nat. Struct. Mol. Biol.* **2011**, *18*, 245–249.
- (59) Fiset, O.; Páslack, C.; Barnes, R.; Isas, J. M.; Langen, R.; Heyden, M.; Han, S.; Schäfer, L. V. Hydration Dynamics of a Peripheral Membrane Protein. *J. Am. Chem. Soc.* **2016**, *138*, 11526–11535.